

Fluid Dynamics in Coal Liquefaction Reactors Using Neutron Absorption Tracer Technique

**Naohide Sakai, Masaki Onozaki, Hitoshi Saegusa, Hirohito Ishibashi, Takashi Hayashi,
and Masatoshi Kobayashi**

Nippon Coal Oil Co., Ltd., Chiyodaku, Tokyo 102-0075, Japan

Noboru Tachikawa and Isamu Ishikawa

Japan Atomic Energy Research Institute, Higashi-Ibaragi-Gun, Ibaragi 311-1313, Japan

Shigeharu Morooka

Kyushu University, Fukuoka 812-8581, Japan

Hydrodynamic properties in the coal liquefaction reactors at the Kashima pilot plant, which was constructed based on the NEDOL process, were investigated using the neutron absorption tracer technique. The reactor system is composed of three vessels, each with 1.0 m ID and 11.8 m in height. The gas velocity in the reactors under coal liquefaction conditions was estimated using a reaction simulator that contained reaction rates and vapor–liquid equilibrium. The axial dispersion coefficients in the first and third reactors at superficial gas velocities of 0.06–0.07 m/s were much smaller than those reported for air–water systems under ambient conditions. This suggests that the pilot-plant reactors operated fundamentally in the homogeneous bubble flow regime.

Introduction

The direct coal liquefaction plant at Kashima, Japan, was designed based on the concept of the NEDOL process, and processes 150 tons of coal per day (Onozaki et al., 2000). The plant is equipped with three reactors, each of which is 1 m in diameter and 11.8 m in length, connected in series. The characterization of the flow properties in the reactors is critically important in terms of analysis of the gas and oil yields produced, as well as for the design of a demonstration plant with a larger production capacity. Gas and liquid holdups and liquid-phase dispersion coefficients in bubble columns for air–water systems have been intensively studied (Deckwer, 1992). The effect of pressure on the hydrodynamics in bubble columns also has been investigated (Wilkinson et al., 1992; Luo et al., 1999; Lin et al., 1999). However, investigations of coal liquefaction reactors of Exxon Donor Solvent process,

EDS (Tarmy et al., 1984), and Solvent Refined Coal process, SRC-II (Panvelker et al., 1982), pilot plants indicate that the flow properties were different from those of bubble columns for air–water systems. The homogeneous bubble flow prevails in coal liquefaction reactors under conditions of high temperature and pressure, while heterogeneous bubble flow or churn turbulent flow prevails for air–water systems at ambient pressure and temperature.

Electrolyte tracers, which are water soluble and frequently used in bubble columns for air–water systems, cannot be used in coal liquefaction reactors. Isotope tracer techniques produce a large quantity of radioactive wastes when they are applied to a large-scale plant, such as the Kashima pilot plant. Thus, a nonradioactive tracer technique, which is based on the interaction of neutrons with tracers (hereafter, referred to as the NAT technique), is desirable since no hazardous wastes are produced during the tests (Clark, 1998). The NAT technique has been applied to the process supporting units of the NEDOL process (PSU; reactor size = 0.175 m ID) at

Correspondence concerning this article should be addressed to Naohide Sakai at the present address: Engineering Section, Environment & Energy Department, Koukan-Keisoku Co., Ltd., 1-1 Minamiwatarida-cho, Kawasaki-ku, Kawasaki-City, Kanagawa 210-0855, Japan.

Kimitsu, Japan (Mochizuki et al., 1997), as well as to a direct coal liquefaction process (Process Development Unit (PDU); reactor size = 0.24 m ID) at Kawasaki, Japan (Ogawa et al., 1987), and a brown coal liquefaction pilot plant (BCL; reactor size = 0.6 m ID) at Victoria, Australia (Tanaka et al., 1992). However, the reactors of the Kashima pilot plant were larger than those of the PSU, PDU and BCL plants. This caused a variety of problems in terms of installations as well as data collection in the case of the Kashima plant. This article reports the essential results of the experiments. Further analysis and discussion are currently under way.

Pilot-Plant Reactors

Table 1 shows the properties of the Tanitoharum coal that was typically processed in the plant. The feed was prepared using pulverized coal, recycled oil, fine-powder pyrite (average diameter = 0.7 μm), and hydrogen-rich recycled gas, and was heated to 660–690 K with a slurry heat exchanger and a fired heater. The coal concentration in the makeup slurry was 40 or 48.5 wt. %. The mixture was heated and introduced into the first reactor through a 107-mm ID upward nozzle. Figure 1 shows a flow chart of the Kashima pilot plant, at which three reactors of 1.0 m ID were installed. The effective height of each reactor was 11.8 m, as calculated by considering the volume of the spherical cap section at the top of the reactor and the conical section at the bottom. The outlet nozzle of the first reactor was connected to the inlet nozzle of the next reactor, and the second one to the third one.

Tracer Tests

Fine-powder gadolinium oxide (Gd_2O_3) (average diameter = 2 μm) was used as the tracer for the neutron absorption. The measuring procedures used at the Kashima pilot plant will be reported in a separate article. A tracer slurry was prepared by suspending the gadolinium powder in the coal oil at a concentration of 50 wt. %. Approximately 0.05–0.06 m^3 of the slurry, which had been stored in the tracer reservoir, was

Table 1. Properties of Tanitoharum Coal

Proximate analysis (dry coal basis)	
Volatile matter	47.0 wt. %
Fixed carbon	48.0 wt. %
Ash	5.0 wt. %
Moisture in feed coal	16.2 wt. %
Ultimate analysis, wt. % (dry ash free basis)	
C: 76.9; H: 5.8; N: 1.9; S: 0.15; O (difference): 15.25	

injected into the feed line to the first or third reactor within 15 s. At the vertical exit line (0.11 m ID) from the first or third reactor, low-energy neutrons were irradiated horizontally using californium-252 as the neutron source. Neutrons were counted using a ^3He -filled proportional counter, which was installed at the opposite side of the pipe from the neutron source, and the neutron intensity was converted to the concentration of the tracer based on calibration curves, which were obtained prior to the measurement. Table 2 shows the operating conditions of the pilot plant when the tracer tests were carried out. Tracer tests were also performed for the case of the cold solvent in order to obtain reference data. The cold solvent contained neither coal fragments nor catalyst particles. The superficial velocity of the gas phase in the reactors under liquefaction conditions were estimated using a simulator, which included the physical properties of the gas and liquid phases, reaction rates, and vapor–liquid equilibrium (Hiraide et al., 1999). Table 3 shows the estimated physical properties of the slurries and the cold solvent under the experimental conditions. The coal particles disintegrated when the makeup slurry was transferred through the heating section. Thus it can be assumed that coal fragments, as well as catalyst and gadolinium particles, are completely and uniformly suspended in the liquid phase, with no slip velocities. Thus the dispersion coefficient of the slurry phase is identical to that of the liquid phase. Hereafter, the slurry phase in the reactor is denoted as the liquid phase for the sake of simplicity.

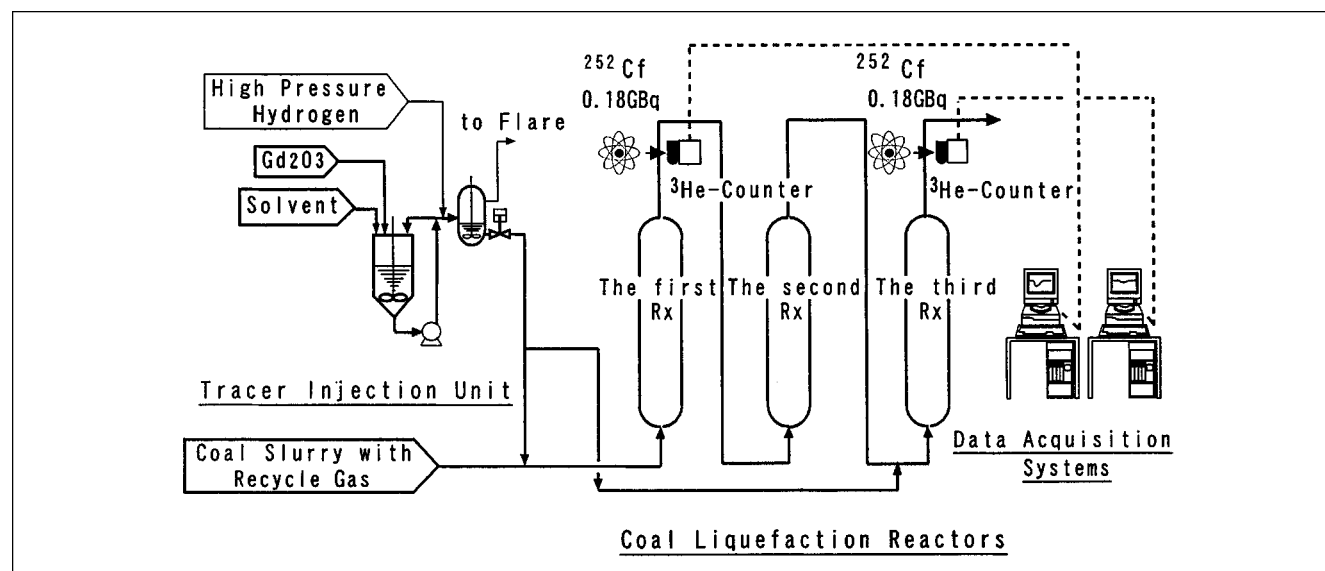


Figure 1. Coal liquefaction system equipped with a NAT apparatus.

Table 2. Operating Conditions and Data for the Kashima Pilot Plant

Operation Mode	Cold Solv. Oper.	40 wt. % Slurry- Liquef. Oper.	48.5 wt. % Slurry- Liquef. Oper.
Makeup slurry			
Slurry feed rate, kg/h	7,800	15,600	12,400
Coal conc. in slurry, wt. % dry coal basis	0	40	48.5
Catalyst (pyrite powder) in slurry, wt. % dry coal basis	0	3	3
Reaction			
Operating pres., MPa	16.6–16.8	16.6–16.8	16.6–16.8
Operating temp. at the top of first reactor, K	313	728	733
Recycle gas/feed slurry,* m ³ (STP)/kg	3.38	0.75	0.96
Yields (daf coal basis), wt. %			
Gas	0	17.2	20.4
Water	0	10.2	9.9
Oil (C4 to bp 811 K fraction)	0	51.0	55.6
Residue (> 811 K fraction)	0	26.1	18.8
Total	0	104.5	104.8
Hydrogen consumption, wt. % dry ash free coal basis	0	4.5	4.8

*(Volumetric flow rate of recycled gas fed to the feed slurry)/(mass flow rate of makeup coal slurry).

Results and Discussion

The residence-time distribution curve of the tracer that is introduced into the reactor as an impulse, $C(t)$, can be described by the following equation.

$$\frac{\partial C(t)}{\partial t} = D_l \cdot \frac{\partial^2 C(t)}{\partial Z^2} - \frac{U_l}{1 - \epsilon} \cdot \frac{\partial C(t)}{\partial Z}, \quad (1)$$

where D_l is the axial dispersion coefficient of liquid, U_l the superficial liquid velocity, and ϵ the gas holdup in the reactor. When the reactor is modeled as a closed vessel, the first and the second moments of the residence-time distribution curve are related to the mean residence time, τ , and the axial dispersion coefficient, D_l , respectively (Levenspiel, 1962):

$$\tau = \Sigma tC(t) / \Sigma C(t) \quad (2)$$

$$\sigma_t^2 = \Sigma t^2 C(t) / \Sigma C(t) - \tau^2 \quad (3)$$

$$\sigma^2 = \sigma_t^2 / \tau^2 = 2/Pe - 2[1 - \exp(-Pe)]/Pe^2 \quad (4)$$

$$D_l = L[U_l/(1 - \epsilon)]/Pe \quad (5)$$

where L is the length of the reactor, which is 11.8 m in the present case.

Table 3. Physical Properties of Gas and Liquid

	Cold Solv. Oper.	40 wt. % Slurry-Liquef. Oper.	48.5 wt. % Slurry-Liquef. Oper.
Coal conc. in slurry, wt. % dry coal basis	0	40	48.5
Gas			
Density, kg/m ³	20	59	62
Viscosity, mPa·s	0.01	0.02	0.02
Liquid			
Density, kg/m ³	960	730	730
Viscosity, mPa·s	7	0.5	0.5

Figures 2, 3, and 4 show normalized residence-time distribution curves, $\phi(t/\tau)$, using the cold solvent, the 40 wt. % slurry, and the 48.5 wt. % slurry, respectively. Data were obtained for each run at the exits of the first and third reactors and were normalized using the mean residence time and the amount of tracer injected. From Eqs. 2–5, the axial dispersion coefficients of the liquid phase in the first and third reactors were determined to be 0.11 m²/s and 0.13 m²/s for the cold-solvent operation, 0.029 m²/s and 0.039 m²/s for the 40 wt. % slurry liquefaction, and 0.022 m²/s and 0.029 m²/s for the 48.5 wt. % slurry liquefaction, respectively. The mean residence time of the liquid phase was also determined for each run, as shown in Table 4. Figures 2–4 also show the residence-time distribution curves, $E(t/\tau)$, calculated from the analytical solution for Eq. 1 with the boundary conditions for a closed vessel (Yagi and Miyauchi, 1955), using the Peclet number determined experimentally from Eqs. 2–5. The measured curves were generally in agreement with the calculated values. However, the experimental value of each dimensionless peak height was higher than the calculated value. This suggests that the flow of the slurry phase in the reactors is not solely diffusional, but is substantially influenced by an internally circulating flow. This aspect remains a topic of future studies.

Figure 5 shows the data of the axial dispersion coefficients of the liquid phase obtained in the present study. The data reported by Tarmy et al. (1984) and Tanaka et al. (1992) in the range of $U_g = 0.04$ – 0.08 m/s are also plotted in the figure. These data were obtained in the coal liquefaction reactors ($D_T = 0.61$ – 0.6 m ID) of the EDS and BCL processes. The axial dispersion coefficients of liquid for air–water systems have been correlated by the following equations.

Kato and Nishiwaki (1972):

$$U_g D_T / D_l = 13 Fr / (1 + 6.5 Fr^{0.8}), \quad (6)$$

where $Fr = (U_g / g D_T)^{0.5}$.

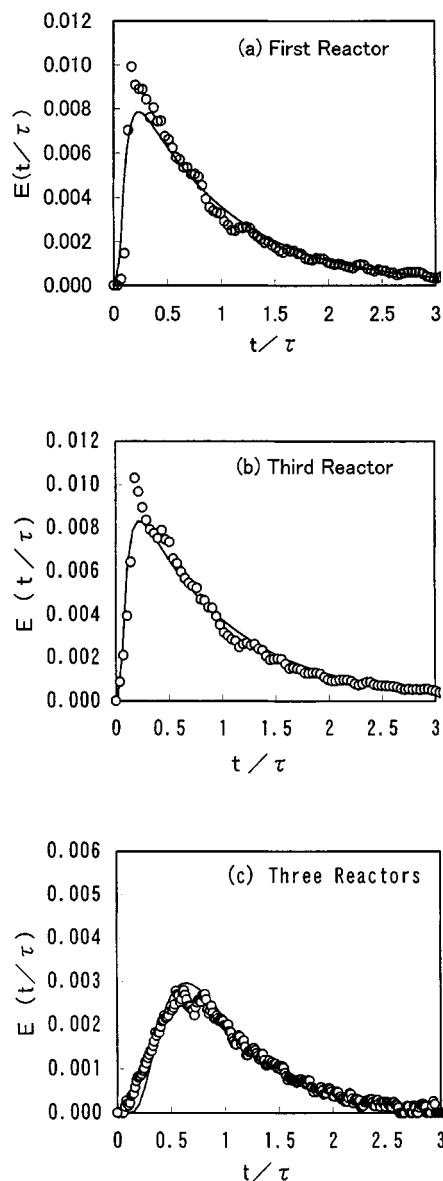


Figure 2. Residence time distributions using cold solvent.

(a) First and (b) third reactors, as well as (c) three reactors connected in series: ○ experimental; — calculated.

Deckwer et al. (1974):

$$D_l = 0.678 D_T^{1.4} U_g^{0.3}, \quad (7)$$

where the axial dispersion coefficient, D_l , is expressed in units of m^2/s , the reactor diameter, D_T , in m, and the superficial gas velocity, U_g , in m/s. Both equations give nearly the same values as shown in Figure 5. The axial dispersion coefficients, which were measured in this study under the liquefaction conditions, are one order of magnitude smaller than those calculated from Eqs. 6 and 7 for air–water systems at ambient pressure and temperature, and 1/3–1/6 of those obtained for the cold solvent. The axial dispersion coefficients in this study are clearly smaller than in the present study,

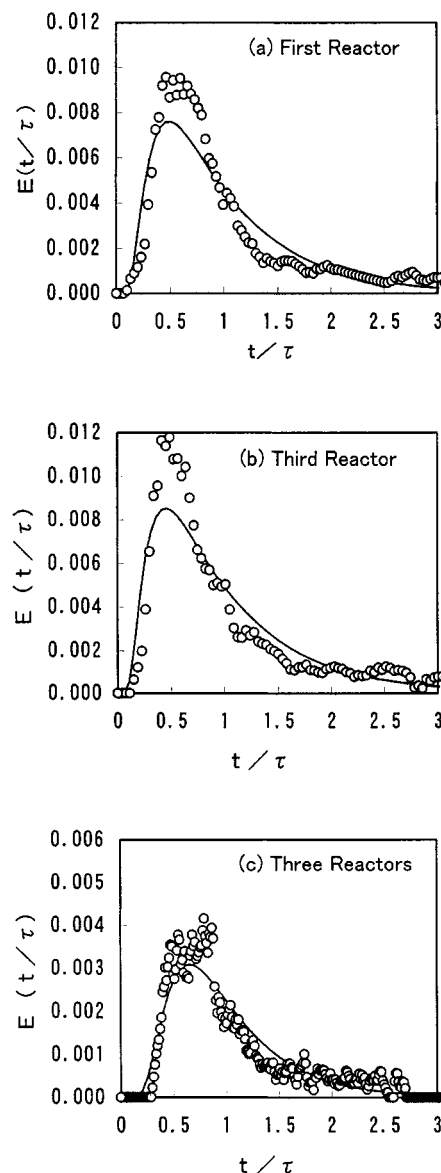


Figure 3. Residence time distribution using a 40 wt. % coal slurry.

(a) First and (b) third reactors, as well as (c) three reactors connected in series: ○ experimental; — calculated.

although they are under nearly the same coal liquefaction conditions. These small axial dispersion coefficients affect the temperature profiles, as well as the sedimentation profiles of grown solid particles, in the liquefaction reactors. Details were reported by Onozaki et al. (2000).

Other important information that was obtained by the tracer tests relates to the mean residence time of the liquid in the reactors. During the liquefaction reaction, oil fractions with lower boiling points vaporize to the gas phase and cease to be in contact with the catalyst particles that are suspended in the liquid. As a result, the residence time of each component in the liquid phase should be estimated from the vapor–liquid equilibrium. However, no reliable data are available for heavy components, although their residence times actually control the oil yield of the reaction. The mean

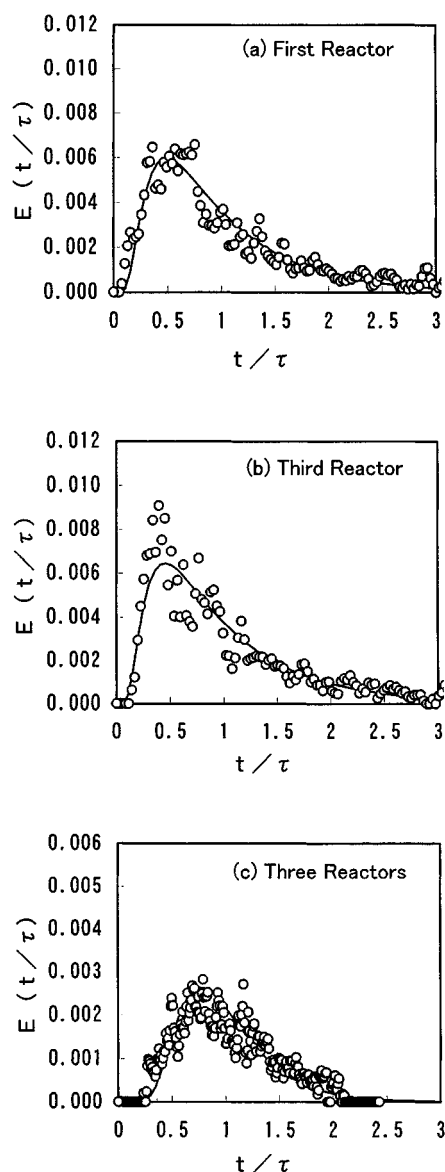


Figure 4. Residence time distribution using a 48.5 wt. % coal slurry.

(a) First and (b) third reactors, as well as (c) three reactors connected in series: ○ experimental; — calculated.

residence time of the gadolinium tracer particles corresponds to that of the heaviest component. The mean residence time through the three reactors was 84 min for the cold solvent operation, 81 min for the 40 wt. % coal slurry liquefaction, and 110 min for the 48.5 wt. % coal slurry liquefaction. These data are useful for the analysis of reaction rates and phase holdups in the reactors.

Conclusions

The axial dispersion coefficients of the liquid phase were determined using the NAT technique under coal liquefaction conditions at the Kashima pilot plant. The values calculated from residence-time distribution curves were in the range of 0.11–0.13 m²/s for the cold solvent operation and 0.02–0.04

Table 4. Fluid Dynamic Characteristics of the Liquefaction Reactors

Operation Mode	Cold Solv. Oper.	40 wt. % Slurry-Liquef. Oper.	48.5 wt. % Slurry-Liquef. Oper.
First reactor			
Mean residence time, min	29	30	38
Variance	0.80	0.49	0.48
Peclet number	0.73	2.7	2.7
Axial dispersion coeff., m ² /s	0.11	0.029	0.022
Third reactor			
Mean residence time, min	28	27	35
Variance	0.81	0.54	0.54
Peclet number	0.66	2.2	2.3
Axial dispersion coeff. m ² /s	0.130	0.039	0.029
Three reactors			
Mean residence time, min	84	81	110
Variance	0.31	0.30	0.18
Peclet number	5.2	5.5	10.0
Axial dispersion coeff. m ² /s	0.050	0.047	0.020

m²/s for the liquefaction operation at superficial gas velocities of 0.06–0.07 m/s. These data were one order of magnitude smaller than the data obtained for air–water systems at ambient pressure and temperature. Data relative to liquid-phase axial dispersion and mean residence time in the reac-

Symbol	Operation	Plant	Investigator
○	cold solvent	BCL, Victoria	Tanaka et al. (1992)
●	liquefaction	BCL, Victoria	Tanaka et al. (1992)
▲	liquefaction	EDS, ECLP	Tarmy et al (1984)
◇	cold solvent	NEDOL, Kashima	this study
◆	liquefaction	NEDOL, Kashima	this study

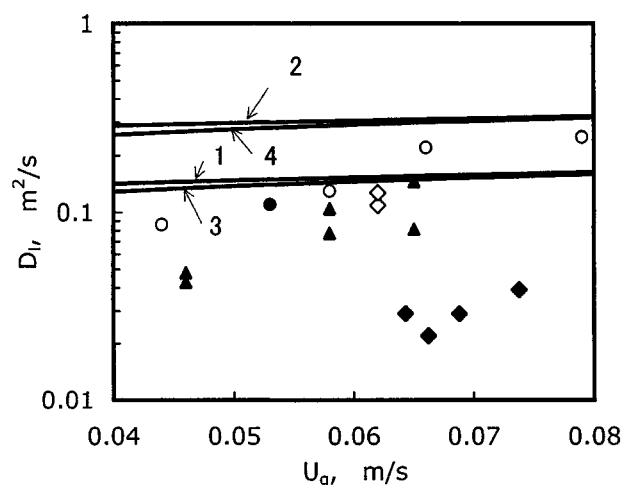


Figure 5. Axial dispersion coefficients.

Calculation: line 1, Eq. 6 for $D_T = 0.61$ m; line 2, Eq. 6 for $D_T = 1.0$ m; line 3, Eq. 7 for $D_T = 0.61$ m; and line 4, Eq. 7 for $D_T = 1.0$ m.

tors under liquefaction conditions can be utilized to analyze the performance of the reactors.

Acknowledgments

This work was funded by the New Sunshine Program of the Agency of Industrial Science and Technology, Ministry of International Trade and Industry. The authors also acknowledge support by the New Energy and Industrial Technology Development Organization (NEDO) and the helpful discussion with Mr. K. Clark, CSIRO, Australia.

Notation

Pe = Peclet number defined by $LU_j/[(1 - \epsilon)D_j]$

t = time, s

z = axial coordinate, m

Literature Cited

- Clark, K., "Progress of the Neutron Absorbing Tracer Studies for Coal Liquefaction," *Proc. Japan/Australia Joint Tech. Meet. on Coal*, Tokyo (1998).
- Deckwer, W.-D., *Bubble Column Reactors*, Wiley, Chichester, England (1992).
- Deckwer, W.-D., R. Burckhart, and G. Zoll, "Mixing and Mass Transfer in Tall Bubble Columns," *Chem. Eng. Sci.*, **29**, 2177 (1974).
- Hiraide, M., H. Itoh, A. Kidoguchi, E. Kaneda, M. Kobayashi, Y. Namiki, Y. Imada, and K. Inokuchi, "Coal Liquefaction Reactor Simulator," *Proc. Int. Symp. Fundamentals for Innovative Coal Utilization*, Sapporo, Japan, p. 103 (1999).
- Kato, Y., and A. Nishiwaki, "Longitudinal Dispersion Coefficient of Liquid in Bubble Column," *Kagaku Kogaku*, **35**, 912 (1971); *Int. Chem. Eng.*, **12**, 182 (1972).
- Levenspiel, O., *Chemical Reaction Engineering*, Wiley, New York (1962).
- Lin, T. J., K. Tsuchiya, and L.-S. Fan, "On the Measurement of Regime Transition in High-Pressure Bubble Columns," *Can. J. Chem. Eng.*, **77**, 370 (1999).
- Luo, X., D. J. Lee, R. Lau, G. Yang, and L.-S. Fan, "Maximum Stable Bubble Size and Gas Holdup in High-Pressure Slurry Bubble Columns," *AIChE J.*, **45**, 665 (1999).
- Mochizuki, M., K. Imada, K. Ikeda, K. Inokuchi, Y. Nogami, T. Takeda, and K. Sakawaki, "Study of Fluid Dynamics in Coal Liquefaction Reactor," *Proc. Japan/German Symp. on Bubble Columns*, Kyoto, Japan (1997).
- Ogawa, T., K. Miyazawa, N. Sasaki, F. Yoshida, and S. Moriguchi, "Studies on Coal and Slurry Properties during Liquefaction," *Proc. Inc. Conf. on Coal Science*, Amsterdam (1987).
- Onozaki, M., Y. Namiki, H. Ishibashi, T. Takagi, M. Kobayashi, and S. Morooka, "Steady-State Thermal Behavior of Coal Liquefaction Reactors Based on NEDOL Process," *Energy & Fuels*, **14**, 355 (2000).
- Panvelker, S. V., J. W. Tierney, Y. T. Shah, and D. F. Rhodes, "Backmixing in a SRC Dissolver," *Chem. Eng. Sci.*, **37**, 1582 (1982).
- Shah, Y. T., *Gas-Liquid-Solid Reactor Design*, McGraw-Hill, New York (1979).
- Tanaka, Y., M. Tamura, H. Kageyama, and K. Clark, "Fluid Dynamics Studies in the Brown Coal Liquefaction Reactor," *Proc. Japan/Australia Joint Tech. Meet. on Coal*, Tokyo, p. 198 (1992).
- Tarmy, B. L., M. Chang, C. A. Coulaloglou, and P. R. Ponzi, "The Three Phase Hydrodynamic Characteristics of the EDS Coal Liquefaction Reactors: Their Development and Use in Reactor Scaleup," *Inst. Chem. Eng. Symp. Ser.*, **87**, 303 (1984).
- Wilkinson, P., A. P. Spek, and L. L. van Dierendonck, "Design Parameters Estimation for Scale-Up of High Pressure Bubble Columns," *AIChE J.*, **38**, 544 (1992).
- Yagi, S., and T. Miyauchi, "Operational Characteristics of the Continuous Flow Reactors in Which the Reactants are Mixing," *Kagaku Kogaku*, **19**, 507 (1955).

Manuscript received May 19, 1999, and revision received Jan. 18, 2000.